This article was downloaded by: *[University of Chicago]*
On: *8 October 2008*
Access details: *Access Details: [subscription number 791985096]*
Publisher *Taylor & Francis*
Informa Ltd Registered in England and Wales Registered Number: 1072954 Registered office: Mortimer House, 37-41 Mortimer Street, London W1T 3JH, UK

High Pressure Research
Publication details, including instructions for authors and subscription information:
http://www.informaworld.com/smpp/title~content=t713679167

Experimental aspects of inelastic X-ray scattering studies on liquids under extreme conditions (P-T)

Ahmet Alatas [a]; Harald Sinn [a]; Jiyong Zhao [a]; Ayman H. Said [a]; Bogdan M. Leu [a]; Wolfgang Sturhahn [a]; Ercan E. Alp [a]; Guoyin Shen [b] Vitali B. Prakapenka [c]et al.
[a] Advanced Photon Source, Argonne National Laboratory, Argonne, IL, USA [b] Geophysical Laboratory, Carnegie Institution of Washington, HPCAT and HPSynC, Argonne, IL, USA [c] Consortium for Advanced Radiation Sources, University of Chicago, Chicago, IL, USA

Online Publication Date: 01 September 2008

To cite this Article Alatas, Ahmet, Sinn, Harald, Zhao, Jiyong, Said, Ayman H., Leu, Bogdan M., Sturhahn, Wolfgang, Alp, Ercan E., Shen, Guoyin Prakapenka, Vitali B.et al.(2008)'Experimental aspects of inelastic X-ray scattering studies on liquids under extreme conditions (P-T)',High Pressure Research,28:3,175 — 183
To link to this Article: DOI: 10.1080/08957950802208928
URL: http://dx.doi.org/10.1080/08957950802208928

PLEASE SCROLL DOWN FOR ARTICLE

Full terms and conditions of use: http://www.informaworld.com/terms-and-conditions-of-access.pdf

This article may be used for research, teaching and private study purposes. Any substantial or systematic reproduction, re-distribution, re-selling, loan or sub-licensing, systematic supply or distribution in any form to anyone is expressly forbidden.

The publisher does not give any warranty express or implied or make any representation that the contents will be complete or accurate or up to date. The accuracy of any instructions, formulae and drug doses should be independently verified with primary sources. The publisher shall not be liable for any loss, actions, claims, proceedings, demand or costs or damages whatsoever or howsoever caused arising directly or indirectly in connection with or arising out of the use of this material.

High Pressure Research
Vol. 28, No. 3, September 2008, 175–183

Taylor & Francis
Taylor & Francis Group

Experimental aspects of inelastic X-ray scattering studies on liquids under extreme conditions (P–T)

Ahmet Alatas[a]*, Harald Sinn[a]†, Jiyong Zhao[a], Ayman H. Said[a], Bogdan M. Leu[a], Wolfgang Sturhahn[a], Ercan E. Alp[a], Guoyin Shen[b] and Vitali B. Prakapenka[c]

[a]*Advanced Photon Source, Argonne National Laboratory, Argonne, IL, USA;* [b]*HPCAT and HPSynC, Geophysical Laboratory, Carnegie Institution of Washington, Argonne, IL, USA;* [c]*Consortium for Advanced Radiation Sources, University of Chicago, Chicago, IL, USA*

(*Received 21 February 2008; final version receiveed 16 May 2008*)

In this study, collective excitations of liquid indium are studied just above the melting point at different pressures (1.7 GPa, 240 °C; 3.0 GPa, 300 °C; 4.0 GPa, 360 °C). The pressures and temperatures are achieved by the use of an externally heated diamond anvil cell. Clear evidence for the existence of propagating modes is observed from the dynamical structure factor at constant momentum transfer (Q) up to about 18 nm^{-1}. The reason for the observed high elastic-scattering background is identified, and its effects on the determination of elastic properties such as viscosity are discussed.

Keywords: inelastic X-ray scattering; collective excitations; liquid indium; diamond anvil cell

Downloaded By: [University of Chicago] At: 18:58 8 October 2008

1. Introduction

Measurement of physical properties of solids or liquids under pressure at high temperatures is important in understanding the behavior of planetary materials. It is clear that any new methodology development will contribute greatly in solving some of the puzzles related to the structure of the Earth and other terrestrial planets, whether this interest originates from a condensed matter physics, mineral physics, or geological viewpoints.

Among the physical properties, the atomic structure is addressed by X-ray diffraction, and great progress has been made in the last two decades in incorporating specially designed diamond anvil cells (DAC) to synchrotron radiation beamlines. A combination of laser heating and resistive heating has expanded our knowledge of the phase diagram and equation of state for many minerals

*Corresponding author. Email: alatas@aps.anl.gov
†Present address: Deutsches Elektronen-Synchrotron, Hasylab, Notkestr. 85, 22607 Hamburg, Germany.

ISSN 0895-7959 print/ISSN 1477-2299 online
This material is published by permission of the Argonne National Laboratory, operated by U. Chicago Argonne, LLC, for the US Department of Energy under Contract No. DE-AC02-06CH11357. The U.S. Government retains for itself, and others acting on its behalf, a paid-up, non-exclusive, and irrevocable worldwide license in said article to reproduce, prepare derivative works, distribute copies to the public, and perform publicly and display publicly, by or on behalf of the Government.
DOI: 10.1080/08957950802208928
http://www.informaworld.com

and alloys at elevated temperatures and pressures reflecting the conditions in the lower mantle, down to the mantle-core boundary [1].

However, the progress in measuring thermo-elastic properties using various inelastic X-ray scattering (IXS) techniques under such extreme conditions has lagged behind; only in the last few years has significant progress been made. Among these attempts, one can mention direct measurement of the phonon density of states with nuclear resonant IXS (NRIXS) [2] or phonon-dispersion relations with momentum-resolved IXS [3–5]. While the measurement of lattice dynamics is relevant to solids, knowledge of viscosity and thermal conductivity are equally relevant and significant to our understanding of the liquid core, as well as the accurate determination of the melting boundary for iron-alloys under core conditions.

The momentum-resolved IXS measures the momentum transfer of the (Q)-dependent energy position, excitation width, and the intensity of Brillouin and Rayleigh peaks. The strength of the Rayleigh (elastic) line is due to the presence of entropy fluctuations in a pure liquid and/or concentration fluctuations and overdamped sound modes, while the Q dependence of the width of the central line is related to thermal conductivity and viscosity. Similarly, the intensity of the Brillouin lines is due to the presence of sustained pressure fluctuations, while the position is related to sound velocity; and the Q-dependence of the width is related to dynamic viscosity. Furthermore, the detailed balance between Stokes and anti-Stokes lines is a good measure of the temperature of the sample, directly measured at the intersection of the X-ray beam and the laser beam [6].

Momentum-resolved IXS has been successfully used in extracting the velocity of sound and viscosity of liquids at ambient pressure and temperature in water [7], alkali metal liquids [8], metal-ammonia solutions [9], and more; see the review article by Scopigno [10]. The regime of very high temperatures exceeding 1500 K was studied for liquid sapphire [11], silicon [12], and titanium [13] by combining the levitation method and the momentum-resolved IXS method. Momentum-resolved IXS measurements of liquids under high pressure and at elevated temperatures are relatively new and more challenging. These challenges are related to the restricted sample environment as well as to signal detection. Momentum-resolved IXS spectra of liquid phosphorus under pressure and temperature were presented to illustrate the potential use of the Paris-Edinburgh large-volume press device [14]. This paper proposes a two-slit collimator system for rejecting parasitic signals coming from the complex sample environment. This slit system, together with a collimator between the detector slit and the analyzer, is a standard setup at sector 3, as will be discussed in Section 3 below. However, more progress is needed in combining heating, DAC, and momentum-resolved IXS techniques simultaneously.

2. Technique

Due to improvements in the source brilliance of third-generation synchrotron radiation sources, coupled with the use of perfect crystal optics for monochromatization of the incident beam and analysis of scattered radiation [15,16], the momentum-resolved IXS technique with few-meV energy resolution has become an important method in condensed matter spectroscopy. Momentum-resolved IXS allows us to study collective excitations as a function of energy and momentum transfer for single crystals, polycrystalline samples, disordered systems, and liquids. The technique is non-destructive and probes the bulk properties of a given structure. It is suitable for a wide range of parameters, *e.g.*, temperature, pressure, and chemical doping.

In principle, the momentum-resolved IXS technique is complementary to inelastic neutron scattering for studying the dynamics in condensed matter physics on mesoscopic-length scales. The main advantages compared with neutron scattering are unlimited access to the energy-momentum

Downloaded By: [University of Chicago] At: 18:58 8 October 2008

space (no kinematic restriction), a purely coherent cross-section, and small beam size on the order of millimeters. Integration of microfocusing optics allows an even smaller beam size of several micrometers [10], which will benefit high-pressure studies.

The kinematic restrictions of neutron scattering prevent reaching acoustic modes over a certain range of wave vector Q and sound velocities larger than $1500\,\mathrm{ms}^{-1}$. In crystals, the translational symmetry of the lattice enables the study of collective excitations in higher Brillouin zones; therefore, the kinematic restriction in the small-Q region can be overcome. However, this is not possible for liquids and disordered systems that have a sound velocity larger than $1500\,\mathrm{ms}^{-1}$, since there is no translational symmetry. The momentum-resolved IXS does not have the kinematic restrictions of neutron scattering; therefore, it is particularly suited to study liquids with high sound velocities [11].

In contrast to Raman and Brillouin spectroscopies, which are limited to studying phonons around the zone center ($Q\sim 0$), momentum-resolved IXS can probe phonons in the entire Brillouin zone, providing information on elastic moduli and elastic anisotropy [4] for single crystals. On the other hand, experiments on polycrystalline samples yield orientationally averaged longitudinal acoustic velocity and bulk properties [17]. Combined with seismic waves and ultrasound measurements, momentum-resolved IXS measurements will provide new insights into geophysically relevant materials.

The spectrometer used for the momentum-resolved IXS technique is state of the art in terms of achievable resolution and intensity in third generation synchrotron facilities. There are five unique spectrometers currently around the world. These are located at the European Synchrotron Radiation Facility (ESRF) in France [18], the Advanced Photon Source (APS) in USA [19], and the Super Photon ring (Spring-8) in Japan [20]. The spectrometers at the ESRF and Spring-8 use a backscattering monochromator to scan the incident energy, whereas the spectrometers at the APS use an in-line monochromator to scan the incident energy [21,22]. As a consequence, the spectrometers at the APS are built in a forward direction, which allows relatively easy integration into a standard beamline design and makes the spectrometers more conducive to incorporate complicated sample environments like levitation heating [11]. Moreover, the in-line monochromator provides the enhanced capabilities of scanning the incident energy.

In general, the liquid dynamical structure factor can be described within the framework of generalized hydrodynamics [23,24] using the memory function approach. It is written as

$$\frac{S(Q,\omega)}{S(Q)} = \frac{1}{\pi}\mathrm{Re}\left[\frac{1}{i\omega + v_{\mathrm{T}}^2 Q^2/(i\omega + M)}\right], \tag{1}$$

where v_{T} is the isothermal sound velocity, ω is the energy of the excitation, and M is the memory function that is responsible for the relaxation process. Different types of memory functions were used in the literature to explain the experimental momentum-resolved IXS spectra, *e.g.*, three-exponential-decay functions accounting for thermal, structural, and microscopic relaxation processes [25] or a Maxwell-type frequency-dependent viscosity with a small non-relaxing part [11]. Detailed information on the dynamical properties of liquids can be found in the recent review article [10].

3. Experiment

The experiment was performed at the Advanced Photon Source beamline 3-ID, and the setup is shown in Figure 1. The synchrotron beam of 21.657 keV is produced by two 2.4-m-long undulators with a 2.7-cm magnetic period. As a premonochromator, water-cooled diamond crystals

Downloaded By: [University of Chicago] At: 18:58 8 October 2008

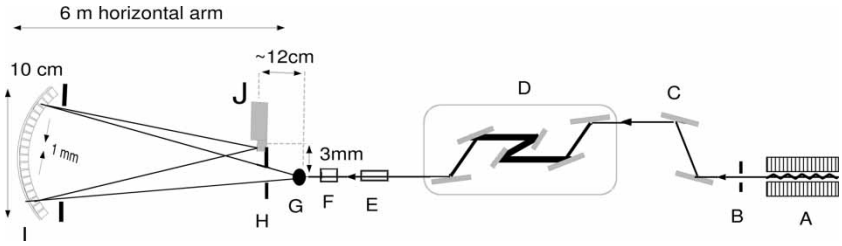

Figure 1. Schematic view of the spectrometer developed at beamline 3-ID. The beam comes from an undulator (A) and premonochromator (C), then passes through the high-resolution monochromator (D) and focusing mirror (E) before it illuminates the sample (G). The scattered intensity is focused by an analyzer (I) into the detector (J). The ionization chamber (F) is used to monitor the incident flux on the sample. The slit systems that determine the source size are (B) and (H). The momentum resolution is determined by an additional slit in front of the analyzer that has a slit opening of $4 \times 10\,\mathrm{cm}^2$ (H × V).

Downloaded By: [University of Chicago] At: 18:58 8 October 2008

are used to reduce the bandwidth to 1.4 eV. The beam is further monochromatized by a cryogenically cooled six-crystal in-line monochromator [22]. The energy transmitted through this high-resolution monochromator has an energy width of ∼1.2 meV. The requirements for very high-energy-resolution optics and the basic principles of such instrumentation are discussed elsewhere [19,21,22,26]. The spectrometer works in the horizontal scattering geometry with a horizontally polarized radiation. The beam is focused $0.25 \times 0.25\,\mathrm{mm}^2$ on the sample by a Pd-coated toroidal mirror. Then the scattered beam is collected by the analyzer for energy selection located 6m from the sample. Currently, four analyzers separated by $3.3\,\mathrm{nm}^{-1}$ in the reciprocal space are used at sector 3. The typical horizontal momentum resolution is $\pm 0.36\,\mathrm{nm}^{-1}$, determined by a 4 cm slit in front of the analyzer. The maximum scattering angle is 18°, which corresponds to a maximum momentum transfer of $34\,\mathrm{nm}^{-1}$. This arrangement allows spectra to be collected simultaneously at four different momentum points. The energy-resolution function of the spectrometer is experimentally determined from a Plexiglass sample at its first static structure maximum. The resolution function was parameterized by a pseudo-Voigt function. The overall energy resolution of the four-analyzer spectrometer is between 2.1–2.3 meV full-width at half-maximum. The resolution is constant over the measured momentum-transfer range within the experimental error ±0.1 meV.

An externally heated DAC (DXR-7, Diacell) is used in this study. The heating of the sample is achieved by inserting four cartridge heaters into the cell body, providing uniform temperature distribution inside the cell. Diamond anvils with 800 μm culet diameter are used. A rhenium gasket is pre-indented to about 100 μm thickness. A 300 μm-diameter hole was drilled in the gasket. Indium powder (99.9999%) together with a small amount of NaCl chips and ruby are loaded into the hole for pressure measurement. From the NaCl diffraction lines, the pressure is determined during the measurement with the use of an image plate detector.

Melting and solidification of the indium sample inside the DAC are observed by the change in the structure factor. The results are shown in Figure 2. The thin black line is the static structure factor of the sample at room temperature. It shows the Bragg peaks of the indium and NaCl. Upon melting, as seen by the thick black line, Bragg peaks from indium have disappeared, and the static structure factor is dominated by a broad peak centered around $23\,\mathrm{nm}^{-1}$. After cooling below the melting temperature (dashed lines), the static structure factor changes back to the room temperature static structure factor curve, but the Bragg reflections from indium are lost. This is due to the growth of single-crystal domains in the sample. During the experiments, the static structure factor $S(Q)$ was measured every 24 hours to verify the quality of the sample and the pressure from the NaCl lines, in addition, to measurements made with the image plate detector. For the 1.7 and 3.0 GPa data sets, we did not observe any changes in the $S(Q)$ scans, ensuring that the sample was intact in the DAC. On the other hand, $S(Q)$ scans taken at 4.0 GPa started to show some changes very close to the end of the experiment. Further investigation was done at

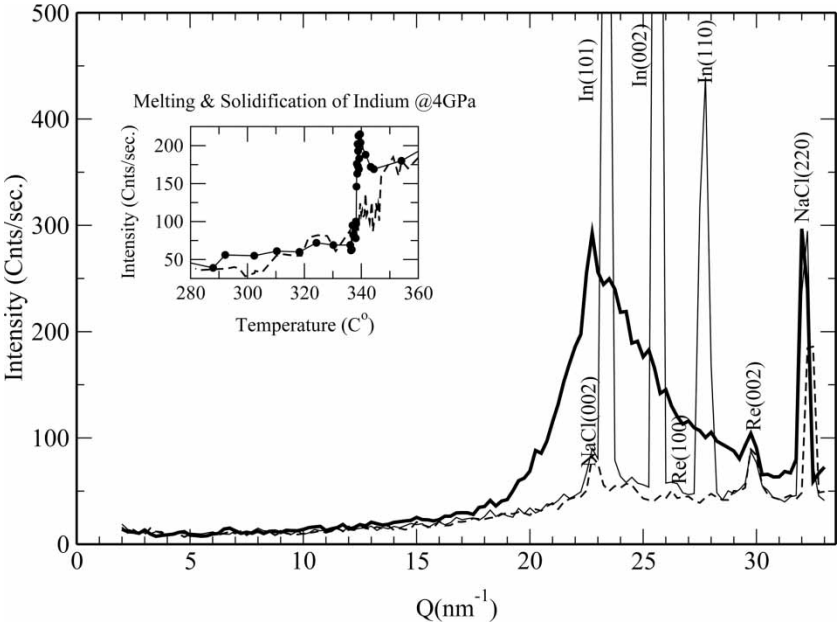

Figure 2. $S(Q)$ scans for powder sample at RT (thin line), liquid sample (thick line), and solid sample at high temperatures (dashed line). Inset shows the melting (circle) and solidification (dashed line) of the sample observed by the change in the structure factor intensities at $Q = 23\,\mathrm{nm}^{-1}$ as a function of temperature at 4 GPa.

room temperature by rocking the sample $\pm 20°$ during the $S(Q)$ scan. It showed an extra Bragg peak compared with the starting material, indicating a change in the composition of the sample. This was also verified by the electron microscope measurement. These data were not included in the evaluation.

The energy scans are shown in Figure 3 as a function of momentum transfers up to $16.15\,\mathrm{nm}^{-1}$ for three different pressure points. Energy scans are achieved by changing the incident energy by rotating the in-line multi-Bragg diffracting high-resolution monochromator crystal, while the

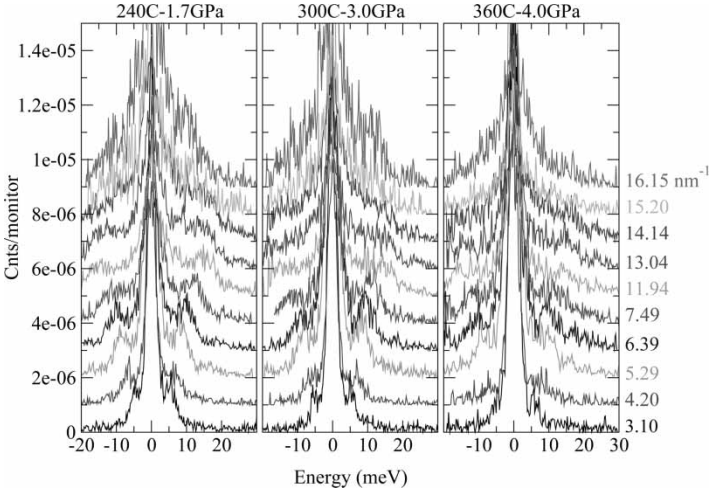

Figure 3. Energy scans for three different pressures as a function of momentum transfer.

Downloaded By: [University of Chicago] At: 18:58 8 October 2008

energies of the excitations are selected by the fixed energy of the analyzers. In these measurements, intensities are normalized to the incoming flux on the sample. The total flux on the sample was 4.5×10^9 photons/s^{-1}/1.2 meV.

4. Results and discussion

Since the energy spectra at low momentum transfer points are dominated by the elastic background as will be discussed below, we did not attempt to analyze data according to Equation (1) to extract thermo elastic quantities. Instead, energy positions and excitation widths were extracted with the damped harmonic oscillator (DHO) model. Dispersion relations and widths are shown in Figure 4. The measured longitudinal sound velocities of the liquid indium at 1.7 and 3.0 GPa do not change significantly within the error bars (2625 ± 60 ms^{-1} at 1.7 GPa and 2610 ± 60 ms^{-1} at 3.0 GPa). For 4.0 GPa, a 10% increase in the sound velocity (2895 ± 60 ms^{-1}) is observed. Sound velocities at 1.7 and 3.0 GPa are about 15% higher than the adiabatic sound velocity [27] and about 10% higher than the longitudinal sound velocity at ambient pressure [25]. Damping can also be explained quantitatively with the mode coupling theory [13], by using $S(Q)$ data from Waseda [28] at ambient pressure and 170 °C.

The relative change in sound velocity as a function of pressure for different materials can be scaled as the ratio of applied pressure to bulk modulus. For example, in the earlier work of Shaw and Caldwell [29], a change of sound velocity as a function of pressure was reported for alkali metals of Na, K, Rb, and Cs. In the absence of electronic transitions, there is a positive monotonic dependence of sound velocity with pressure. The relative change in sound velocity of liquid alkali metals at pressures corresponding to 10% of their solid bulk modulus varies between 14% and 21% [29]. Similarly, we find a 12% change in the sound velocity of liquid indium at 4 GPa, corresponding to 10% of its solid bulk modulus. In order to make an exact comparison, correct values of the temperature-dependent bulk modulus would be needed to scale the applied pressure with the material's compressibility. Such a baseline would enable us to determine anomalies due to electronic or structural phase transitions taking place in the liquid state.

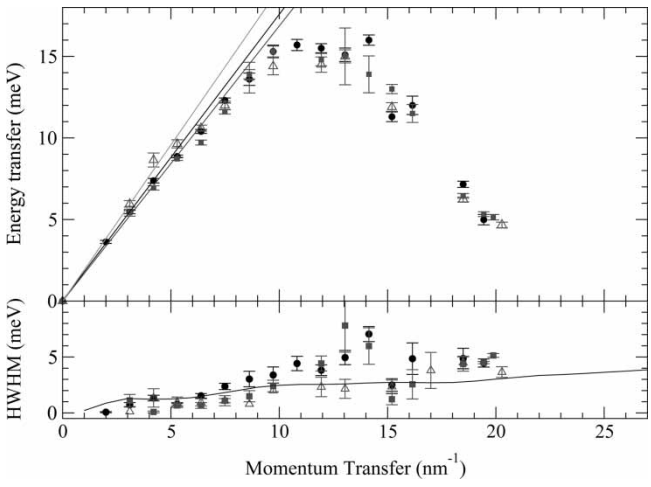

Figure 4. Dispersion of the collective excitations for different pressures and temperatures. Circles, squares, and triangles represent the data for 1.7 GPa, 240 °C, 3.0 GPa, 300 °C, and 4.0 GPa, 360 °C, respectively. From the slope of the dispersion curves, longitudinal sound velocities are calculated as 2625 ± 60 ms^{-1} at 1.7 GPa, 2610 ± 60 ms^{-1} at 3.0 GPa, and 2895 ± 60 ms^{-1} at 4.0 GPa. The width of the excitations are also included in the figure together with mode coupling fitting using $S(Q)$ data obtained from Waseda [28].

Downloaded By: [University of Chicago] At: 18:58 8 October 2008

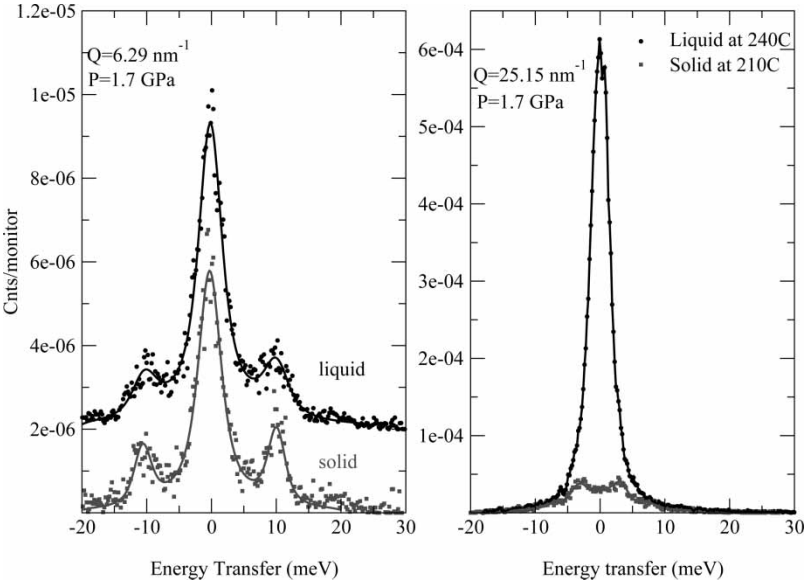

Figure 5. Energy scans for liquid (circles) and hot-solid (squares) indium at two different Q points. Solid lines are fitted to data. Liquid data at 6.29 nm^{-1} are vertically shifted for clarity.

Energy scans were also performed for the hot solid sample just below the melting point to determine background scattering at each momentum transfer point. These are shown in Figure 5 for two momentum points at 6.29 and 25.15 nm^{-1}. Their fitting parameters are given in Table 1. At 6.29 nm^{-1}, both liquid and hot solid energy spectra show almost the same strength for elastic peaks compared with the relatively low elastic background level for the liquid at 25.15 nm^{-1}. At this point, comprehension of how much of the elastic peak comes from the surrounding environment of the sample especially from diamonds is necessary. This is important since the scattering volume includes a 2 mm thick diamond for momentum transfers up to 34 nm^{-1}. This scattering volume is defined by the incident beam size and the 2 mm detector slits located 12 cm away from the sample, as shown in Figure 6 for two different scattering angles (2° and 15°). A rhenium gasket blocks the scattering from the diamond located on the upstream side. On the other hand, the diamond located on downstream side contributes to the scattering volume even at 15°.

The momentum-resolved IXS technique can be used to measure the longitudinal viscosity in liquids, which is difficult to access with traditional contact measurements for viscosity. Since the viscosity is related to the inverse of the width of the central peak within the visco-elastic theory (at finite frequencies and wave vectors) [10,11,13], it is very important that the elastic

Table 1. Fitting parameters for spectra at 6.29 and 25.15 nm^{-1}. Integrated intensity, width, and position of the peaks are represented by I,Γ, and ω, respectively. Central and side peaks are represented by the subscripts 0 and s.

	Liquid at 6.29 nm^{-1}	Solid at 6.29 nm^{-1}	Liquid at 25.15 nm^{-1}	Solid at 25.15 nm^{-1}
Total monitor counts	18.5 Million/200 s	9.3 Million/100 s	3.7 Million/40 s	1.8 Million/20 s
$I_0(\times 10^{-5})$	4.66 ± 0.125	3.65 ± 0.129	286 ± 1.27	10.1 ± 6.92
Γ_0(meV)	1.33 ± 0.08	1.28 ± 0.1	0.7 ± 0.009	1.92 ± 0.9
ω_0(meV)	−0.28 ± 0.05	−0.38 ± 0.06	0.013 ± 0.009	−0.2 ± 0.06
$I_s(\times 10^{-5})$	0.21 ± 0.016	0.183 ± 0.014		1.06 ± 0.23
Γ_s(meV)	1.53 ± 0.2	0.61 ± 0.15		0.78 ± 0.22
ω_s(meV)	10.4 ± 0.12	10.4 ± 0.1		3.46 ± 0.08
χ^2	0.77	1.00	1.81	0.87

Downloaded By: [University of Chicago] At: 18:58 8 October 2008

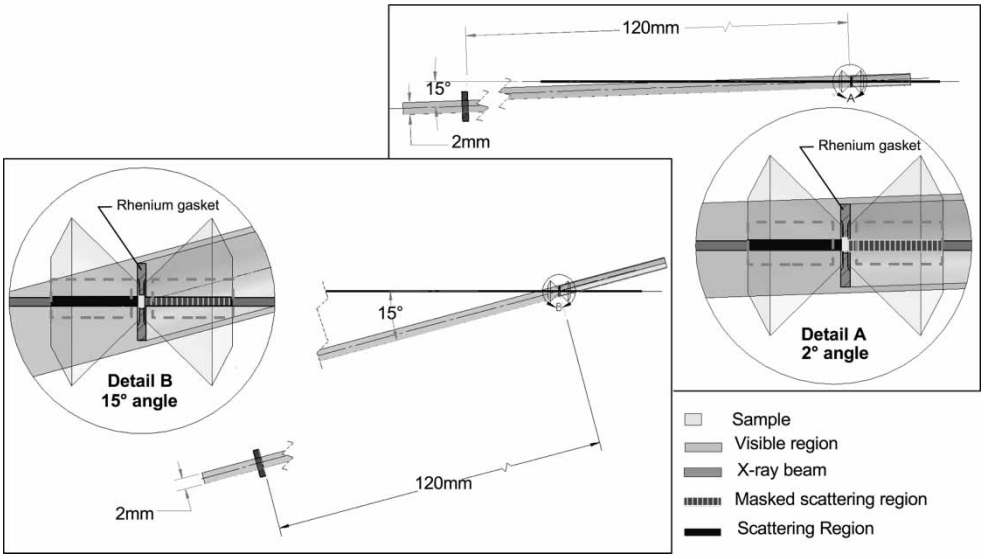

Figure 6. The scattering volume as seen by the 2 mm slits located at 120 mm away from sample for two scattering angles at 2° and 15°. Inset figures are magnified for clear views of the sample environment. Scattering volume is defined by the cross section of the incident beam and scattering as seen by the analyzer restricted by the detector pinhole and the rhenium gasket. The dashed lines on the diamond represent the proposed perforated diamonds that will reduce scattering from the diamond.

Downloaded By: [University of Chicago] At: 18:58 8 October 2008

background from diamond scattering is properly subtracted. To reduce the elastic background from the diamond scattering, one can use perforated diamonds, which would minimize the scattering volume occupied by the diamond (as shown in Figure 6 with dashed lines), and use a collimator between the cell and the detector slit. The collimator will allow only those scattered beams that have the correct scattering angle and will better define the scattering volume. Another way to overcome this problem is the use of a Paris-Edinburgh-type multi-anvil cell, although this also has its own limitations as explained in [14]. This type of cell can be applied to materials with low-Z elements, which would increase the absorption length.

IXS is a very promising technique for studying thermo-elastic properties of liquids under pressure relevant to geophysical science. We have demonstrated the feasibility of such experiments, identified the problems related to the experimental setup and data analysis, and discussed ways to overcome these problems.

Acknowledgements

The use of the Advanced Photon Source was supported by the US Department of Energy, Office of Science, Office of Basic Energy Sciences, under Contract No. DE-AC02-06CH11357. The high pressure devices in the research were supported by NSF grant no. 0738852 (to G.S.). The electron microscopy was accomplished at the Electron Microscopy Center for Materials Research at the Argonne National Laboratory, a US Department of Energy, Office of Science Laboratory operated under contract no. DE-AC02-06CH11357 by UChicago Argonne, LLC. We would like to thank R.E. Cook of ANL for the help with using the electron microscope and B. Brajuskovic of APS for providing Figure 6.

References

[1] G. Shen, H.K. Mao, R.J. Hemley, T.S. Duffy, and M.L. Rivers, *Melting and crystal structure of iron at high pressures*, Geophys. Res. Lett. 25 (1998), pp. 373–376.

[2] H.K. Mao, J. Xu, V.V. Struzhkin, J. Shu, R.J. Hemley, W. Sturhahn, M.Y. Hu, E.E. Alp, L. Vocadlo, D. Alfé, G. Price, M. Gillan, M. Schwoerer-Böhning, D. Häusermann, P. Eng, G. Shen, H. Giefers, R. Lübbers, and G. Wortmann, *Melting and crystal structure of iron at high pressures*, Science 292 (2001), pp. 914–916.

[3] D. Antonangeli, F. Occelli, H. Requardt, J. Badro, G. Fiquet, and M. Krisch, *Elastic anisotropy in textured hcp-iron to 112 GPa from sound wave propagation measurements*, Earth Planetary Sci. Lett. 225 (2004), pp. 243–251.
[4] D. Antonangeli, M. Krisch, G. Fiquet, D.L. Farber, C.M. Acacne, J. Badro, F. Occelli, and H. Requardt, *Elasticity of cobalt at high pressure studied by inelastic X-ray scattering*, Phys. Rev. Lett. 93 (2004), p. 215505.
[5] G. Fiquet, J. Badro, F. Guyot, C. Bellin, M. Krisch, D. Antonangeli, H. Requardt, A. Mermet, D.L. Farber, C. Acacne-Ruddle, and J. Zhang, *Application of inelastic X-ray scattering to the measurements of acoustic wave velocities in geophysical materials at very high pressure*, Phys. Earth Planet. Inter. 143–144 (2004), pp. 5–18.
[6] J.F. Lin, W. Sturhahn, J. Zhao, G. Shen, H.K. Mao, and R.J. Hemley, *Absolute temperature measurement in a laser-heated diamond anvil cell*, Geophys. Res. Lett. 31 (2004), p. L14611.
[7] G. Monaco, A. Cunsolo, G. Ruocco, and F. Sette, *Viscoelastic behavior of water in the terahertz-frequency range: an inelastic x-ray scattering study*, Phys. Rev. E 60 (1999), pp. 5505–5521.
[8] H. Sinn, F. Sette, U. Bergmann, C. Halcoussis, M. Krisch, R. Verbeni, and E. Burkel, *Coherent dynamic structure factor of liquid lithium by inelastic X-ray scattering*, Phys. Rev. Lett. 78 (1997), pp. 1715–1718.
[9] C.A. Burns, P.M. Platzman, H. Sinn, A. Alatas, and E.E. Alp, *Evidence for an instability near twice the Fermi wave vector in the low electronic density liquid metal* $Li(NH3)4$, Phys. Rev. Lett. 86 (2001), pp. 2357–2360.
[10] T. Scopigno, G. Ruocco, and F. Sette, *Microscopic dynamics in liquid metals: the experimental point of view*, Rev. Mod. Phys. 77 (2005), pp. 881–933.
[11] H. Sinn, B. Glorieux, L. Hennet, A. Alatas, M. Hu, E.E. Alp, F.J. Bermejo, D.L. Price, and M.-L. Saboungi, *Microscopic dynamics of liquid aluminum oxide*, Science 299 (2003), pp. 2047–2049.
[12] A. Alatas, A.H. Said, H. Sinn, E.E. Alp, C.N. Kodituwakku, B. Reinhart, M.-L. Saboungi, and D.L. Price, *Elastic modulus of supercooled liquid and hot solid silicon measured by inelastic X-ray scattering*, J. Phys. Chem. Solids 66 (2005), pp. 2230–2234.
[13] A.H. Said, H. Sinn, A. Alatas, C.A. Burns, D.L. Price, M.-L. Saboungi, and W. Schirmacher, *Collective excitations in an early molten transition metal*, Phys. Rev. B 74 (2006), p. 172202.
[14] S. Falconi, G. Monaco, W.A. Crichton, M. Mezouar, and R. Verbeni, *Collimator for inelasic x-ray scattering experiments at high temperature and pressure conditons*, High Press. Res. 24 (2004), pp. 463–469.
[15] E. Burkel, *Phonon spectroscopy by inelastic x-ray scattering*, Rep. Prog. Phys. 63 (2000), p. 171.
[16] M. Krisch and F. Sette, *Inelastic X-ray scattering from phonons*, *Light Scattering in Solids IX, Topics Appl. Physics*, Vol. 108, Springer-Verlag, Berlin, Heidelberg, 2007, pp. 317–370.
[17] A. Bosak, M. Krisch, I. Fischer, S. Huotari, and G. Monaco, *Inelastic x-ray scattering from polycrystalline materials at low momentum transfer*, Phys. Rev. B 75 (2007), p. 092302.
[18] F. Sette, G. Ruocco, M. Krisch, U. Bergmann, C. Masciovecchio, V. Mazzacurati, G. Signorelli, and R. Verbeni, *Collective dynamics in water by high energy resolution inelastic X-ray scattering*, Phys. Rev. Lett. 75 (1995), pp. 850–853.
[19] H. Sinn, E.E. Alp, A. Alatas, J. Barraza, G. Bortel, E. Burkel, D. Shu, W. Sturhahn, J. Sutter, T. Toellner, and J. Zhao, *An inelastic X-ray spectrometer with 2.2 meV energy resolution*, Nucl. Instrum. Methods Phys. Res. Sec. A 467–468 (2001), p. 1545.
[20] A. Baron, Y. Tanaka, D. Miwa, D. Ishikawa, T. Mochizuki, K. Takeshita, S. Goto, T. Matsushita, H. Kimura, F. Yamamoto, and T. Ishikawa, *Early commissioning of the SPring-8 beamline for high resolution inelastic X-ray scattering*, Nucl. Instrum. Methods Phys. Res. Sec. A 467 (2001), pp. 627–630.
[21] T.S. Toellner, *Monochromatization of synchrotron radiation for nuclear resonant scattering experiments*, Hyperfine Interact. 125 (2000), pp. 3–28.
[22] T.S. Toellner, A. Alatas, A. Said, D. Shu, W. Sturhahn, and J. Zhao, *A cryogenically stabilized meV-monochromator for hard X-rays*, J. Synchrotron Radiat. 13 (2006), pp. 211–215.
[23] U. Balucani and M. Zoppi, *Dynamics of the Liquid State*, Clarendon, New York, 1983.
[24] J. Boon and S. Yip, *Molecular Hydrodynamics*, McGraw-Hill, New York, 1980.
[25] H. Reichert, F. Bencivenga, B. Wehinger, M. Krisch, F. Sette, and H. Dosch, *High-frequency subsurface and bulk dynamics of liquid indium*, Phys. Rev. Lett. 98 (2007), p. 096104.
[26] E. Burkel, *Inelastic Scattering of X-Rays with Very High Energy Resolution*, 2nd ed., *Springer Tracts in Modern Physics*, Vol. 125, Springer-Verlag, Berlin, Heidedelberg, New York, 1991.
[27] Y. Tsuchiya, *Compressibility of the liquid indium-antimony system*, J. Phys. Soc. Japan 66 (1997), pp. 120–124.
[28] Y. Waseda, *The Structure of non-Crystalline Materials*, McGraw-Hill, New York, 1980; S(Q) data are available online at: http://www.tagen.tohoku.ac.jp/general/building/iamp/database/scm/LIQ/sq.html; accessed 25 April 2007.
[29] G.H. Shaw and D.A. Caldwell, *Sound-wave velocities in liquid alkali metals studied at temperatures up to* 150° *and pressures up to* 0.7 *GPa*, Phys. Rev. B 32 (1985), pp. 7937–7947.

Downloaded By: [University of Chicago] At: 18:58 8 October 2008